

Mapping Pigmentation in Human Skin by Multi-Visible-Spectral Imaging by Inverse Optical Scattering Technique

Norimichi Tsumura, Miki Kawabuchi, Hideaki Haneishi, and Yoichi Miyake
Department of Information and Image Sciences, Chiba University,
Chiba, Japan

Abstract

Mapping pigmentation in human skin is expected to give useful information in reproducing and diagnosing various skin colors. In this research, maps of melanin, oxy-hemoglobin and deoxy-hemoglobin in skin are estimated from multi-visible-spectral image by using an inverse optical scattering technique. In the inverse optical scattering technique, first of all, a forward model of optical scattering is build to simulate the spectral reflectance of skin. Changing the variable parameters in the forward model, the simulation is repeated until the simulated spectral reflectance matches with the spectral reflectance at each pixel of the multi-spectral image. The principle of the proposed estimation technique was confirmed by imaging the human forearm under the venous occlusion, the venous and arterial occlusion, and by imaging a slapped region of the human forearm.

Introduction

Extracting qualitative information and spatial distribution of components such as pigmentation through analyzing an observed image is required in many fields of image analysis such as remote sensing, medical diagnostics, and robot vision. Spectral characteristics of the components are useful information to identify the components, because different materials have different spectroscopic responses to electromagnetic waves of a certain energy band. A technique that uses a spectral image as an observed image was proposed¹ and has been expected to lead the field of image analysis.

Skin color reproduction may be considered the most important problem in color reproduction of color film and color television systems. With the recent progress of various imaging systems²⁻⁴ such as multimedia, computer graphic and telemedicine systems, skin color becomes increasingly important for communication, image reproduction on hardcopy and softcopy, medical diagnosis, cosmetic development and so on. Human skin is a turbid medium with multi-layered structure,^{5,6} and various pigments such as melanin and hemoglobin are contained in

the medium. Slight changes in structure and pigment construction produce rich skin color variation. Therefore, it is necessary to analyze skin color on the basis of the structure and pigment construction in reproducing and diagnosing various skin colors.

We have already proposed a technique to extract the map of skin pigmentation from skin color images⁷ or skin spectral absorbance image⁸ by independent component analysis. The facial color images were separated into the images that correspond to distribution of melanin and hemoglobin. The separated components were synthesized to simulate the various facial color images by changing the quantities of the two separated pigments. In the analysis of skin color, it was assumed that the linearity among the quantities of pigment and the observed color signals holds in the optical density domain. However, the optical scattering in skin which causes the broad distribution of optical path length histogram in the skin may violate the linearity. It was also assumed that spectral absorbance of the pigment will not change spatially. However, hemoglobin has two type of state: oxy-hemoglobin(HbO_2), and deoxy-hemoglobin(Hb), and ratio between HbO_2 and Hb will change spatially in a large area of skin image or in an area of skin diseases. The oxygen saturation is defined by the ratio between oxy-hemoglobin and total hemoglobin. Mapping oxygen saturation of blood in skin will give useful information for skin diagnosis.⁹

In this paper, the pigmentations of melanin, oxy-hemoglobin and deoxy-hemoglobin in skin are estimated from multi-visible-spectral image by using the inverse optical scattering technique. The reflected visible light will provide information only for epidermis and dermis layers in the skin, because most of visible light does not penetrate into subcutis layer. The principle of the proposed estimation technique was confirmed by imaging the human forearm under venous occlusion, venous and arterial occlusion, and by imaging a slapped region of the human forearm.

In the inverse optical scattering technique, first of all, a forward model of optical scattering is build to simulate the spectral reflectance of the skin. Changing the variable parameters in the forward model, the simulation is repeated until the simulated spectral reflectance matches with the

spectral reflectance at each pixel of the multi-spectral image. The conventional non-linear optimization technique is used to change the variable parameters at each iteration.

In the next section, the forward model of optical scattering in human skin is described. The inverse optical scattering technique is explained based on the forward model. Finally, the experimental results of imaging the human forearm under venous and arterial occlusions, and imaging a slapped region of the human forearm are shown.

Forward Model of Optical Scattering in Skin

Monte Carlo Simulation for Light Transport in Multi-Layered Tissue

Lihong Wang and Steven L. Jacques made an excellent Standard C-code for Monte Carlo simulation for light transport in multi-layered tissue.¹⁰ The program is called MCML. In this research, the MCML program is used to simulate the spectral reflectance on the skin. Figure 1 shows an example of the Monte Carlo simulation which was used by Lihong Wang and Steven L. Jacques. Each step between photon positions is variable and equals $-\ln(\xi) / (\mu_a + \mu_s)$ where ξ is a random number and μ_a and μ_s are absorption and scattering coefficients, respectively. The value of g which is the anisotropy factor of scattering is used to decide an angle of deflection. The weight of the photon is decreased from an initial value of 1 as it moves through the tissue, and equals a^n after n steps, where a is the albedo ($a = \mu_s / (\mu_a + \mu_s)$). When the photon strikes the surface, a fraction of the photon weight escapes as reflectance and remaining weight is internally reflected and continue to propagate. Many photon trajectories are calculated to yield a statistical description of photon distribution in the medium. The ratio between the sum of weights that escape from the surface and sum of initial weights used in the simulation gives the diffuse reflectance.

Three-Layered Model of Human Skin and its Spectral Reflectance by Monte Carlo Simulation

Figure 2 shows the three-layered model of skin, which is composed of the epidermis, dermis and subcutis layers. In this model, it is supposed that the skin color is dominated by the concentration of melanin in the epidermis layer, oxy-hemoglobin and deoxy-hemoglobin in the dermis layer. The refractive index in air and tissue are set for 1.0 and 1.4 respectively. The depths of epidermis, dermis and subcutis layers are set for 0.007 cm, 0.113 cm, and 0.5 cm respectively. The scattering coefficient and anisotropy factor used in epidermis and dermis layers are shown in Fig. 3, which were published by Germert et al.¹¹ The scattering coefficient and anisotropy factor in subcutis layer are set for 600 [cm^{-1}] and 0.8 in all wavelengths respectively. The absorption cross sections of melanin μ_a^{melanin} , oxy-hemoglobin $\mu_a^{\text{HbO}_2}$ and deoxy-hemoglobin μ_a^{Hb} are shown in Fig. 4, which were published by Anderson et al.¹² In this research, variable parameters in the skin model are the only concentrations of melanin c^{Melanin} , oxy-hemoglobin c^{HbO_2} and deoxy-hemoglobin c^{Hb} .

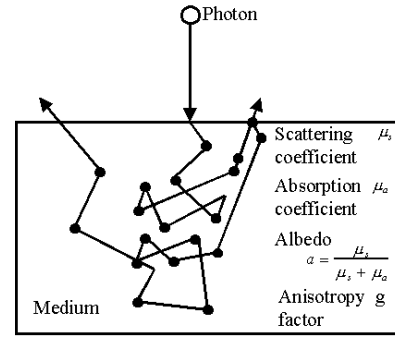


Figure 1 The movement of one photon through a homogenous medium, as calculated by Monte Carlo simulation.

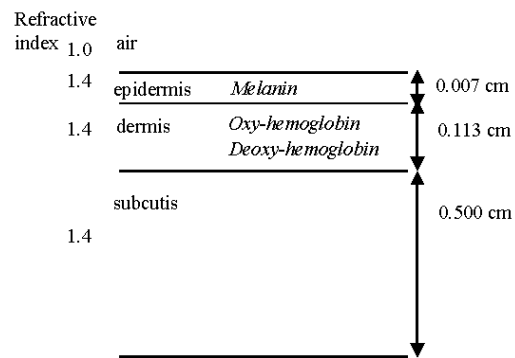


Figure 2 Three layered model of skin

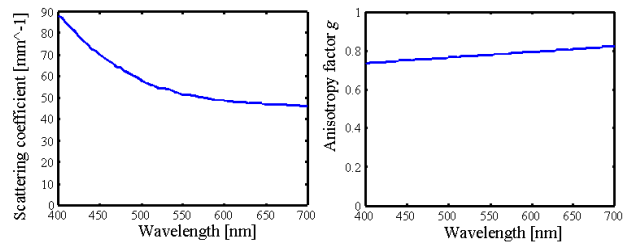


Figure 3 Scattering coefficient and anisotropy factor in epidermis and dermis layer

The Monte Carlo simulation in this three-layered skin model is easily performed by using MCML program. It is required to run the program for each wavelength to obtain the spectral reflectance. One million photons were used for each wavelength. To evaluate the error of simulation, it was repeated 10 times changing the initial random value. Figure 5(a) shows the resultant averaged spectral reflectance for 10 times simulations, where the concentrations of melanin, oxy-hemoglobin and deoxy-hemoglobin were set to 150, 9, 1 [$\times 10^{-5}$ mol/L] respectively. The standard deviation of error in each wavelength for 10 data is shown in

Fig. 5(b). It is shown that the deviation of Monte Carlo simulation is under 3.5×10^{-4} in all wavelengths.

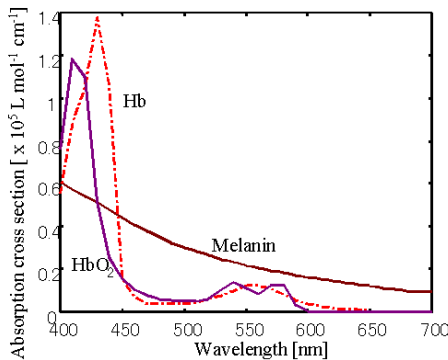


Figure 4 Absorption cross section of melanin, oxy-hemoglobin (HbO_2), and deoxy-hemoglobin (Hb)

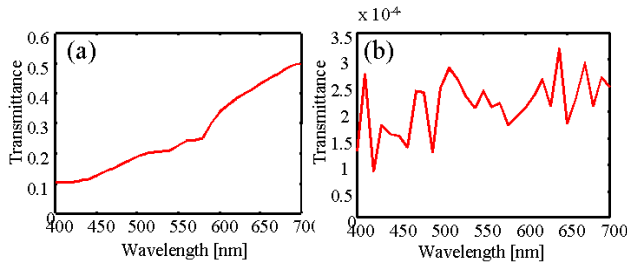
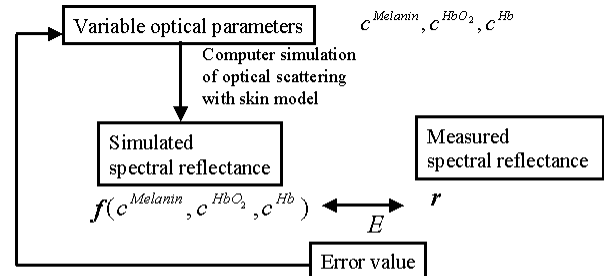


Figure 5(a) Result of Monte Carlo simulation and (b) Standard deviation of error in the simulation

Inverse Optical Scattering Technique

The concentration of pigments is estimated from diffuse spectral reflectance. Figure 6 shows the schematic diagram of the estimation method. At first, the initial values of variable parameters $c^{Melanin}$, c^{HbO_2} , c^{Hb} are randomly given, and the spectral reflectance is simulated using the initial parameters based on the forward model of optical scattering in human skin. The amount of error is calculated between the simulated spectral reflectance and measured spectral reflectance. If the error is not small enough, the variable parameters are changed, and spectral reflectance is simulated again by using the changed parameters. If the error is small enough, the parameters used for the simulation are results of the estimation. To decide the change of parameters, a conventional optimization technique is used by MATLAB optimization tool box¹³. In this research, we used the reflectance on 580 nm, 610 nm and 640 nm wavelength for the estimation. Figure 7 shows examples of the estimation. In Fig. 7(a), concentrations of melanin and total hemoglobin are set for 150×10^{-5} mol/L, 10×10^{-5} mol/L, respectively. The saturation is changed from 0.0 to 1.0. The horizontal axis indicate the target saturation value for the estimation, vertical axis indicate the estimated saturation value by the above method. In Fig. 7(b), concentrations of

total hemoglobin and saturation are set for 10×10^{-5} mol/L, 0.9 respectively. The concentrations of melanin are changed from 0 to 300×10^{-5} mol/L. In Fig. 7(c), concentrations of melanin and saturation are set for 150×10^{-5} mol/L, 0.9 respectively. The concentrations of hemoglobin are changed from 0 to 30×10^{-5} mol/L. These results show that the concentrations and saturation are successfully estimated by the proposed technique.



If E is not minimized, parameters are modified based on optimization technique.
If E is minimized, the parameters are the estimated parameters.

Figure 6 Estimation of concentrations of pigments from diffuse spectral reflectance

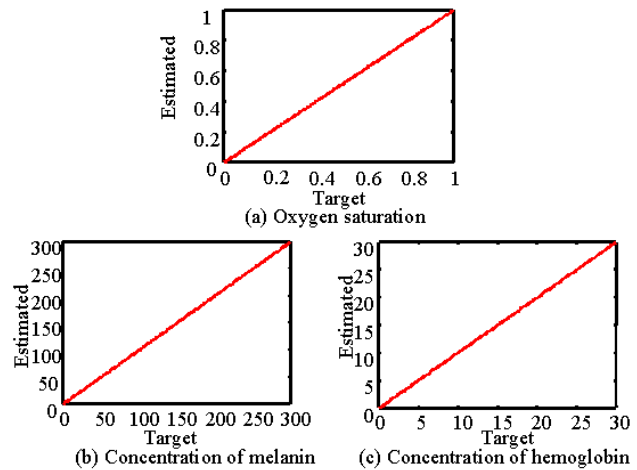


Figure 7 Results of estimation of concentrations of pigments from absolute diffuse spectral reflectance

Experiments

The imaging system consists of standard white-light source (Natural Light NL-500, USHI/MURAKAMI) and a multi-spectral camera (OLYMPUS).⁴ A wheel with 10 interference color filters is rotating between the lens and monochromatic CCD in the multi-spectral camera. The peak wavelengths of filter transmittance are arranged between 430nm~700nm in 30 nm intervals. In our experiment, only three color filters; 580, 610, 640 nm are used for the estimation of pigmentation. A reference white diffuse reflectance plate was placed on the skin and was used to

calibrate the imaging system. During the occlusions in the elbow, the skin image in the forearm was captured every 30 seconds. The occlusions were continued for 3 minutes. After releasing the occlusions, the skin image was captured every 30 seconds. Figure 8 shows the results of experiment.

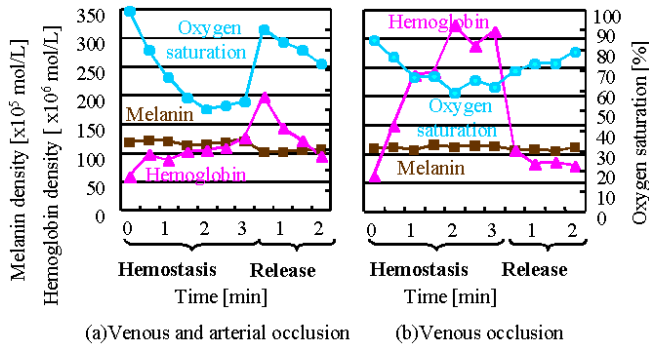


Figure 8 Results of estimation of concentrations of pigments from imaging the human forearm under (a) venous and arterial occlusion, (b) venous occlusion

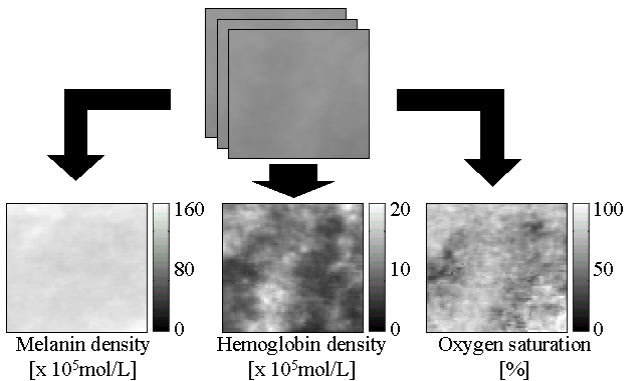


Figure 9 Results of estimation of concentrations of pigments from imaging the slapped region of the human skin.

The oxygen saturation decreases more rapidly and decreases to a lower level for venous and arterial occlusion than for venous occlusion. On the other hand, the blood volume increases more rapidly and increases to a higher level for venous occlusion than for venous and arterial occlusion. The estimated concentration of melanin was almost constant during and after the occlusions. Since these results agree with physiological data, we think that the proposed technique is an effective means for estimating the 2-D distribution of the relative value of oxygen saturation, blood volume and pigmentation in the skin area. By imaging a slapped region of the human forearm, the increase of oxygen saturation and blood volume were imaged by our estimation technique as shown in Fig. 9.

Conclusion

The maps of melanin, oxy-hemoglobin and deoxy-hemoglobin in skin are estimated from multi-visible-spectral image by using the inverse optical scattering technique. Influences of noise, 3-D shape, specularly should be investigated in further investigations. However, the results show a possibility to diagnose a skin disease by multi-visible-spectral imaging, and resultant map will give useful information in reproducing various skin colors.

References

1. S. Kawata, K. Sasaki and S. Minami, "Component analysis of spatial and spectral patterns in multispectral images. I. Basis," *Journal of the Optical Society of America A* 4, 2101-2106 (1987).
2. F.H. Imai, N. Tsumura, H. Haneishi and Y. Miyake, "Principal component analysis of skin color and its application to colorimetric color reproduction on CRT display and hardcopy," *J. Image Science and Technology* 40, 422-430 (1996).
3. Y. Yokoyama, N. Tsumura, H. Haneishi, Y. Miyake, J. Hayashi and M. Saito, "A new color management system based on human perception and its application to recording and reproduction of art printing," in *Proceedings of IS&T/SID's 5th Color Imaging Conference, Color Science, Systems and Appl.* (Society for Imaging Science & Technology, Springfield, VA, 1997) pp. 169-172 .
4. M. Yamaguchi, R. Iwama, Y. Ohya, T. Obi, N. Ohya and Y. Komiya, "Natural color reproduction in the television system for telemedicine," in *Medical Imaging 1997: Image Display*, Y. Kim, ed., *Proc. Soc. Photo-Opt. Instrum. Eng.* 3031, 482-489 (1997).
5. M.J.C.van Gemert, S.L. Jacques, H.J.C.M. Sternborg and W.M. Star, "Skin optics," *IEEE Trans. on Biomedical Engineering* 36, 1146-1154 (1989).
6. R.R. Anderson and J.A. Parrish, "The optics in human skin," *The Journal of Invest. Dermatology* 77, 13-19 (1981).
7. N. Tsumura, H. Haneishi and Y. Miyake, "Independent component analysis of skin color image," *Journal of the Optical Society of America A* 16, pp. 2169-2176 (1999).
8. N. Tsumura, H. Haneishi and Y. Miyake, "Independent component analysis of skin absorbance image," *Optical Review* (Submitted).
9. P.J. Dwyer, R.R. Anderson and C.A. DiMarzio, "Mapping blood oxygen saturation using a multi-spectral imaging system," in *Biomedical Sensing, Imaging, and Tracking Technologies II*, T. Vo-Dinh, R. A. Lieberman, and G. G. Vurek, eds., *Proc. Soc. Photo-Opt. Instrum. Eng.* 2976, 270-280 (1997).
10. Wang, L., Jacques, S. L., Monte Carlo Modeling of Light Transport in Multi-layered Tissues in Standard C, University of Texas M. D. Anderson Cancer Center, 1992.
11. Gemert, M.J.C.V., Jacques, S. L., Sternborg, H. J. C. M. and Star, W.M., *Skin optics*, *IEEE Trans on Biomed. Eng.* 36, 1146, 1989.
12. Anderson R. R., Parrish, J. A., *The optics of human skin*, *The Journal of Investigative Dermatology* 77, 13, 1981.
13. A. Garce. *Matlab Optimization Toolbox User's Guide* (The Math Works, Boston, MA, 1992).